Letter

Shedding new light on $\mathcal{R}(D_{(s)}^{(*)})$ and $|V_{cb}|$ from semileptonic $\bar{B}_{(s)} \to D_{(s)}^{(*)} \ell \bar{\nu}_\ell$ decays

Bo-Yan Cui,[*] Yong-Kang Huang,[†] Yu-Ming Wang,[‡] and Xue-Chen Zhao[§]
School of Physics, Nankai University, Weijin Road 94, Tianjin 300071, People's Republic of China

(Received 22 February 2023; revised 26 August 2023; accepted 25 September 2023; published 20 October 2023)

We compute for the first time the next-to-leading-order QCD corrections to the $\bar{B}_{(s)} \to D_{(s)}^{(*)}$ form factors at large hadronic recoil. Both the charm-quark-mass- and the strange-quark-mass- dependent pieces can generate the leading-power contributions to these form factors. Including further various power-suppressed contributions, we perform the combined fits of the considered form factors to both our large-recoil theory predictions and the lattice QCD results, thus improving upon the previous determinations of the lepton-flavor-universality ratios $\mathcal{R}(D^{(*)})$ significantly.

DOI: 10.1103/PhysRevD.108.L071504

I. INTRODUCTION

The flagship semileptonic $\bar{B}_{(s)} \to D_{(s)}^{(*)} \ell \bar{\nu}_\ell$ decay processes are of extraordinary phenomenological importance for the precise determination of the Cabibbo-Kobayashi-Maskawa (CKM) matrix element $|V_{cb}|$ and for probing the nonstandard flavor-changing dynamics above the electroweak scale [1–6]. The persisting discrepancy between the exclusive and inclusive extractions of $|V_{cb}|$ has triggered enormous efforts on uncovering the ultimate mystery of this intriguing puzzle in the Standard Model (SM) and beyond [7–11]. Moreover, the state-of-the-art theory predictions for the two lepton-flavor-universality (LFU) ratios $\mathcal{R}(D^{(*)})$ [12] appear to be in tension with the HFLAV-averaged experimental measurements [13] as well, thus stimulating intensive investigations on a wide range of other interesting LFU observables [14–22]. Apparently, disentangling the potential new physics (NP) signals from the unaccounted theoretical uncertainties in the SM computations in a robust manner will be indispensable for the unambiguous interpretation of these emerged flavor anomalies. It remains important to remark that the updated LHCb measurements for the electron-muon universality rations $\mathcal{R}(K^{(*)})$ in the flavor-changing neutral current loop processes $B \to K^{(*)} e^+ e^-$ and $B \to K^{(*)} \mu^+ \mu^-$ [23,24] do not necessarily lead to conclude the tauon-muon universality in the neutral current $b \to s \ell \bar{\ell}$ transitions [25,26], let alone in the flavor-changing charged current tree decays $\bar{B}_{(s)} \to D_{(s)}^{(*)} \ell \bar{\nu}_\ell$ [27]. Actually, introducing new CP-violating couplings in the weak effective Hamiltonian for $b \to s \ell \bar{\ell}$ can bring about the significant space to violate the electron-muon universality, while accommodating the new LHCb result for the $\mathcal{R}(K)$ ratio simultaneously [28].

The model-independent descriptions of the heavy-to-heavy bottom-meson decay form factors in the low recoil regime can be naturally formulated by adopting the heavy quark effective theory (HQET) based upon an expansion in powers of $\Lambda_{\rm QCD}/m_{b,c}$. In order to better constrain the desirable shape of these form factors, an attractive prescription to derive the unitarity constraints for the form-factor expansion coefficients has been developed from the fundamental field-theoretical principles [29–34]. Additionally, we have witnessed the substantial progress on the encouraging lattice QCD calculations of the $\bar{B} \to D^{(*)} \ell \bar{\nu}_{\bar{\ell}}$ form factors [35–37] and the $\bar{B}_s \to D_s^{(*)} \ell \bar{\nu}_{\bar{\ell}}$ form factors [38–40] at nonzero recoil. By contrast, the continuum QCD determinations of such fundamental heavy-to-heavy form factors at large recoil are mainly achieved by evaluating only the leading-order QCD contributions at the twist-four accuracy [41,42], apart from the currently available higher-order QCD computations of the $\bar{B} \to D$ form factors [43,44].

In view of the noticeable significance of implementing the large-recoil theory predictions in the numerical fit of the exclusive bottom-meson decay form factors [45–54], accomplishing the next-to-leading-order (NLO) computations to the semileptonic $\bar{B}_{(s)} \to D_{(s)}^{*} \ell \bar{\nu}_{\bar{\ell}}$ form factors will therefore be in high demand for pinning down the obtained

[*]boyancui@nankai.edu.cn
[†]huangyongkang@mail.nankai.edu.cn
[‡]Corresponding author: wangyuming@nankai.edu.cn
[§]Corresponding author: zxc@mail.nankai.edu.cn

uncertainties of their shape parameters from the combined z-series fitting procedure. To achieve this goal, we will first establish the NLO factorization formulas for the appropriate bottom-meson-to-vacuum correlation functions at leading power (LP) in the soft-collinear effective theory (SCET) framework and then construct the large logarithmic resummation improved light-cone sum rules (LCSR) for the considered form factors. In particular, we will report on a novel observation of the LP $\mathcal{O}(\alpha_s)$ contribution to the longitudinal form factors due to the unsuppressed charm-quark-mass-dependent pieces in the SCET Lagrangian, when applying the preferable power-counting scheme $m_c \sim \mathcal{O}(\sqrt{\Lambda_{\rm QCD} m_b})$ [55,56]. Phenomenological implications of the simultaneous Boyd-Grinstein-Lebed (BGL) expansion fitting [29–31] to both the SCET sum rules predictions and the lattice simulation data points will be further explored with the focus on the updated extractions of the LFU quantities $\mathcal{R}(D^{(*)}_{(s)})$ and the CKM matrix element $|V_{cb}|$.

II. GENERAL ANALYSIS

We adopt the customary definitions of the form factors $\{V, A_0, A_1, A_2\}$ as displayed in [57]. Implementing the QCD → SCET$_{\rm I}$ matching for these form factors enables us to derive the following factorization formulas:

$$\begin{aligned}
\mathcal{V}(n\cdot p) &= C_V^{(\rm A0)}(n\cdot p)\xi_\perp(n\cdot p) + C_V^{(\rm A1,m_c)}(n\cdot p)\xi_{\perp,m_c}(n\cdot p) + \int_0^1 d\tau C_V^{(\rm B1)}(\tau,n\cdot p)\Xi_\perp(\tau,n\cdot p) + \mathcal{V}^{\rm NLP}(n\cdot p),\\
\mathcal{A}_0(n\cdot p) &= C_{f_0}^{(\rm A0)}(n\cdot p)\xi_\parallel(n\cdot p) + C_{f_0}^{(\rm A1,m_c)}(n\cdot p)\xi_{\parallel,m_c}(n\cdot p) + \int_0^1 d\tau C_{f_0}^{(\rm B1)}(\tau,n\cdot p)\Xi_\parallel(\tau,n\cdot p) + \mathcal{A}_0^{\rm NLP}(n\cdot p),\\
\mathcal{A}_1(n\cdot p) &= C_V^{(\rm A0)}(n\cdot p)\xi_\perp(n\cdot p) + C_{A_1}^{(\rm A1,m_c)}(n\cdot p)\xi_{\perp,m_c}(n\cdot p) + \int_0^1 d\tau C_V^{(\rm B1)}(\tau,n\cdot p)\Xi_\perp(\tau,n\cdot p) + \mathcal{A}_1^{\rm NLP}(n\cdot p),\\
\mathcal{A}_{12}(n\cdot p) &= C_{f_+}^{(\rm A0)}(n\cdot p)\xi_\parallel(n\cdot p) + C_{f_+}^{(\rm A1,m_c)}(n\cdot p)\xi_{\parallel,m_c}(n\cdot p) + \int_0^1 d\tau C_{f_+}^{(\rm B1)}(\tau,n\cdot p)\Xi_\parallel(\tau,n\cdot p) + \mathcal{A}_{12}^{\rm NLP}(n\cdot p). \qquad (1)
\end{aligned}$$

The form factors $\mathcal{V}$, $\mathcal{A}_0$, $\mathcal{A}_1$, and $\mathcal{A}_{12}$ can be expressed in terms of the conventional form factors as displayed in (1) of the Supplemental Material [58]. The explicit definitions of $\xi_{\parallel,\perp}$ and $\Xi_{\parallel,\perp}$ take the same form as the ones for the exclusive heavy-to-light transitions [59], while $\xi_{\parallel,m_c}$ and $\xi_{\perp,m_c}$ can be defined by

$$\langle D_q^*(p,\epsilon^*)|(\bar\xi W_c)\frac{\not{\bar n}}{2}\frac{m_c}{-i n\cdot \overleftarrow{D}_c}\gamma_5 h_v|\bar B_v\rangle = -n\cdot p(\epsilon^*\cdot v)\xi_{\parallel,m_c}(n\cdot p), \qquad (2)$$

$$\langle D_q^*(p,\epsilon^*)|(\bar\xi W_c)\frac{\not{\bar n}}{2}\frac{m_c}{-i n\cdot \overleftarrow{D}_c}\gamma_5\gamma_{\mu\perp} h_v|\bar B_v\rangle = -n\cdot p(\epsilon^*_\mu - \epsilon^*\cdot v\bar n_\mu)\xi_{\perp,m_c}(n\cdot p). \qquad (3)$$

The analytic expressions for the short-distance coefficients $C_i^{(\rm A0)}$ and $C_i^{(\rm B1)}$ [60,61] as well as $C_i^{(\rm A1,m_c)}$ are collected in (2) of the Supplemental Material [58]. We will therefore dedicate the next section to the transparent computations of the effective form factors.

III. NLO CORRECTIONS TO THE FORM FACTORS

In analogy to the strategy for computing the heavy-to-light bottom-meson decay matrix elements [62,63] (see also [64,65]), we can derive the LCSR for $\xi_\parallel(n\cdot p)$ by exploring the particular SCET$_{\rm I}$ correlation function

$$\begin{aligned}
\Pi_{\nu,\parallel}^{(\rm A0)} &= \int d^4x e^{ip\cdot x}\langle 0|{\rm T}\{j^{(2)}_{\xi q,\parallel\nu}(x), O_\parallel^{(\rm A0)}(0)\}|\bar B_v\rangle + \int d^4x e^{ip\cdot x}\int d^4y\langle 0|{\rm T}\{j^{(0)}_{\xi\xi,\parallel\nu}(x), i\mathcal{L}^{(2)}_{\xi q}(y), O_\parallel^{(\rm A0)}(0)\}|\bar B_v\rangle\\
&+\int d^4x e^{ip\cdot x}\int d^4y\int d^4z\langle 0|{\rm T}\{j^{(0)}_{\xi\xi,\parallel\nu}(x), i\mathcal{L}^{(1)}_{\xi q}(y), i\mathcal{L}^{(0)}_{\xi m_c}(z), O_\parallel^{(\rm A0)}(0)\}|\bar B_v\rangle\\
&+\int d^4x e^{ip\cdot x}\int d^4y\langle 0|{\rm T}\{j^{(0)}_{\xi\xi,\parallel\nu}(x), i\mathcal{L}^{(2)}_{\xi q,m_q}(y), O_\parallel^{(\rm A0)}(0)\}|\bar B_v\rangle, \qquad (4)
\end{aligned}$$

where the manifest representations of $j^{(0)}_{\xi\xi,\parallel\nu}$, $j^{(2)}_{\xi q,\parallel\nu}$, $\mathcal{L}^{(1)}_{\xi q}$, and $\mathcal{L}^{(2)}_{\xi q}$ have been presented in [57,66]. The remaining effective Lagrangian densities and the SCET$_{\rm I}$ weak current are presented in (3) of the Supplemental Material [58]. Since the charm-quark-mass-dependent term $\mathcal{L}^{(0)}_{\xi m_c}$ describes the unsuppressed interaction between the collinear fields [67], the third term in the correlation function (4) will result in the power-enhanced contribution to *the correlation* *function* (4). Moreover, the spectator-quark mass contributions from the second and the fourth terms on the right-hand side of (4) can further give rise to the LP effects (see also [46,67,68]).

Matching the determined spectral representation of $\Pi_{\nu,\parallel}^{(\mathrm{A0})}$ with the corresponding hadronic dispersion relation leads to the desired NLO sum rules

$$\xi_\parallel = 2\frac{\mathcal{F}_{B_q}(\mu)}{f_{D_q^*,\parallel}}\frac{m_{B_q}m_{D_q^*}}{(n\cdot p)^2}\int_0^{\omega_s} d\omega' \exp\left[\frac{m_{D_q^*}^2 - n\cdot p\omega'}{n\cdot p\omega_M}\right] \times\left[\phi_{B,\mathrm{eff}}^-(\omega') - \frac{m_c}{\omega'}\phi_{B,\mathrm{eff}}^{+,m_c}(\omega') + \frac{m_q}{\omega'}\phi_{B,\mathrm{eff}}^{+,m_q}(\omega')\right] \equiv \hat{\xi}_\parallel + \hat{\xi}_\parallel^{m_c} + \hat{\xi}_\parallel^{m_q}. \quad (5)$$

The lengthy expressions for $\phi_{B,\mathrm{eff}}^-$, $\phi_{B,\mathrm{eff}}^{+,m_c}$ and $\phi_{B,\mathrm{eff}}^{+,m_q}$ are summarized in the Supplemental Material [58]. Remarkably, the $\mathrm{SCET_I}$ diagram (b) in Fig. 1 of the Supplemental Material does not lead to the power-enhanced contribution (but does generate the LP contribution) to the sum rules of $\xi_\parallel$ after implementing *the continuum subtraction*.

Applying the established strategy further allows for the construction of the SCET sum rules for the effective form factors $\xi_{\parallel,m_c}$, $\Xi_\parallel$, $\xi_\perp$, $\xi_{\perp,m_c}$, and $\Xi_\perp$ as collected in the Supplemental Material [58]. We then proceed to construct the subleading-power sum rules for $\mathcal{V}^{\mathrm{NLP}}$, $\mathcal{A}_0^{\mathrm{NLP}}$, $\mathcal{A}_1^{\mathrm{NLP}}$, and $\mathcal{A}_{12}^{\mathrm{NLP}}$ at tree level, which will be presented explicitly in a forthcoming longer write-up.

IV. NUMERICAL ANALYSIS

We continue to explore phenomenological implications of the SCET sum rules with the three-parameter *Ansätz* for the bottom-meson distribution amplitudes [69] (see also [70–76]), which fulfills simultaneously the nontrivial equations-of-motion constraints [69], the sum rule determinations of the two inverse moments $\lambda_{B_{d,s}}$ [77,78] and the HQET parameters $\lambda_{E,H}^2$ [79–81], and the asymptotic behaviors at small quark and gluon momenta [82]. It is perhaps worth mentioning an attractive method for the first-principles determination of the B-meson distribution amplitude based upon the large momentum effective theory [83]. The leptonic decay constants of the pseudoscalar bottom mesons have been extracted from the lattice calculations precisely [84]. We further employ the QCD sum rule computations [85] for the D_q^* decay constants. The allowed intervals of the intrinsic LCSR parameters $M^2 = n\cdot p\omega_M$ and $s_0 = n\cdot p\omega_s$ are consistent with the previous determinations [86–89]. The choices for the additional parameters in numerical studies are identical to the ones summarized in [46].

Inspecting the numerical features in Fig. 1, the particular charm-quark-mass-dependent contribution $\hat{\xi}_\parallel^{m_c}$ in (5) can bring about the $\mathcal{O}(5\%)$ enhancement of the LP prediction

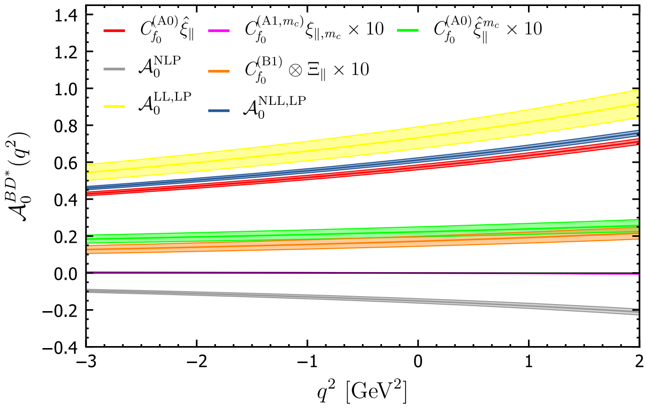

FIG. 1. Breakdown of the distinct dynamical mechanisms contributing to the form factor $\mathcal{A}_0$ for $\bar{B}\to D^*\ell\bar{\nu}_\ell$ in the kinematic range $q^2\in[-3.0, 2.0]$ GeV^2 with the uncertainties from varying the hard and hard-collinear matching scales.

of the form factor $\mathcal{A}_0$ with $q^2\in[-3.0, 2.0]$ GeV^2. We further note that the effective form factor $\xi_{\parallel,m_c}$ defined in (2) can only result in the negligible impact at large hadronic recoil due to the kinematical suppression of the multiplication hard coefficient. In order to determine the mean values and theoretical uncertainties of the $\bar{B}_q\to D_q^*$ form factors, we employ the statistical procedure discussed in [90,91] by simultaneously scanning the complete set of input parameters in the adopted intervals. It is worthwhile mentioning further that the systematic uncertainty due to the parton-hadron duality *Ansätz* has been addressed in a wide range of QCD computations (e.g., [92–101]), leading to the encouraging observation on the smallness of duality violations in the inclusive hadron production in e^+e^- annihilations [100], in the hadronic decays of the τ-lepton [101], and in the semileptonic bottom-meson decays [98]. In an attempt to obtain more conservative predictions of our SCET sum rules, we nevertheless increase the default intervals of M^2 and s_0 by a factor of 2 in the ultimate error estimates. The principal benefit of our LCSR analysis consists in the strong correlations between the LCSR data points at distinct q^2-values, which are expected to be particularly insensitive to the duality approximation.

In order to extrapolate the LCSR predictions for the $\bar{B}_q\to D_q^*$ form factors toward the large momentum transfer, we will apply the BGL parametrization [29–31] as widely employed in the form-factor determinations (see, for instance, [47,48,102]) and then perform the binned χ^2 fit of our LCSR predictions at $q^2\in\{-3.0, -2.0, -1.0, 0.0, 1.0, 2.0\}$ GeV^2, in combination with the lattice QCD results. Moreover, we will implement the strong unitarity constraints on the BGL coefficients b_n^i by including all the $\bar{B}_q^{(*)}\to D_q^{(*)}$ channels.

Combining the LCSR results for the $\bar{B}_q\to D_q^*$ form factors with (i) the SCET sum rules for the $\bar{B}_q\to D_q$ form factors [44], (ii) the lattice results for the $\bar{B}\to D$

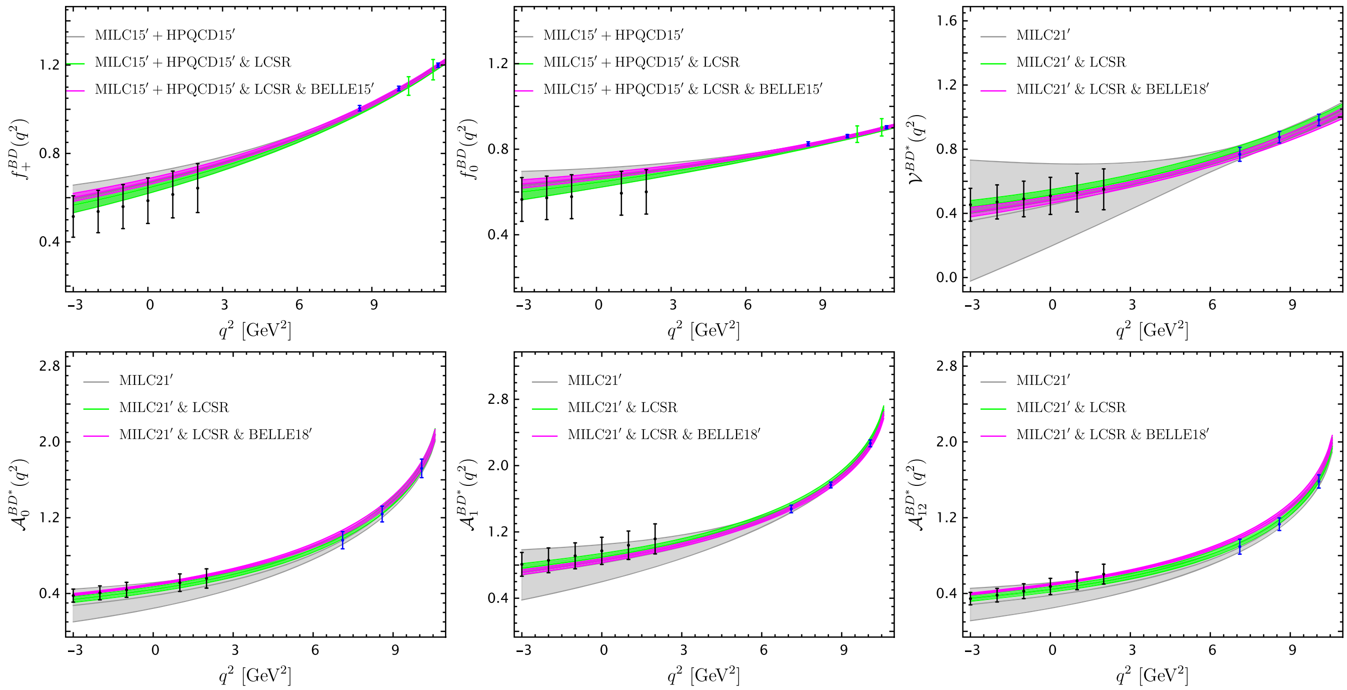

FIG. 2. The determined momentum-transfer dependence of the $\bar{B} \to D^{(*)}$ form factors in the entire kinematic region from (i) the BGL fit against the "only lattice QCD" data points [35–37,39,40], (ii) the simultaneous fit to both the lattice QCD results [35–37,39,40] and our LCSR predictions, and (iii) the combined fit including further the experimental data points [1,3–5].

TABLE I. The determined z-series coefficients of the $\bar{B}_q \to D_q^{(*)}$ form factors from the BGL fitting against the "only lattice QCD" data points [35–37,39,40] (shown in the second and the fifth columns), from the simultaneous fitting to both the lattice QCD results [35–37,39,40] and the LCSR computations (shown in the third and the sixth columns), and from implementing further the experimental data points [1,3–5] in the BGL fit procedure (shown in the fourth and the last columns).

	$\bar{B} \to D^{(*)}$ form factors			$\bar{B}_s \to D_s^{(*)}$ form factors		
Parameters	Lattice	Lattice ⊕ LCSR	Lattice ⊕ LCSR ⊕ Exp	Lattice	Lattice ⊕ LCSR	Lattice ⊕ LCSR ⊕ Exp
$b_0^{f_+}$	0.0137 ± 0.0001	0.0137 ± 0.0001	0.0138 ± 0.0001	0.0041 ± 0.0001	0.0041 ± 0.0001	0.0042 ± 0.0001
$b_1^{f_+}$	-0.0414 ± 0.0034	-0.0417 ± 0.0033	-0.0398 ± 0.0032	-0.0029 ± 0.0019	-0.0030 ± 0.0019	-0.0034 ± 0.0015
$b_2^{f_+}$	0.1178 ± 0.2007	0.0415 ± 0.1124	0.1123 ± 0.0713	-0.0584 ± 0.0096	-0.0588 ± 0.0093	-0.0608 ± 0.0078
$b_1^{f_0}$	-0.2064 ± 0.0155	-0.2072 ± 0.0147	-0.2004 ± 0.0144	-0.0610 ± 0.0112	-0.0617 ± 0.0111	-0.0571 ± 0.0108
$b_2^{f_0}$	0.5572 ± 0.9626	0.1880 ± 0.5330	0.5581 ± 0.3297	-0.0264 ± 0.0768	-0.0233 ± 0.0767	-0.0359 ± 0.0756
b_0^g	0.0259 ± 0.0009	0.0256 ± 0.0009	0.0251 ± 0.0008	0.0080 ± 0.0009	0.0072 ± 0.0007	0.0071 ± 0.0007
b_1^g	-0.1093 ± 0.0786	-0.1005 ± 0.0456	-0.1104 ± 0.0396	0.0212 ± 0.0218	-0.0017 ± 0.0106	-0.0005 ± 0.0105
b_2^g	-0.4505 ± 4.3691	0.2587 ± 0.6564	0.2050 ± 0.6107	-0.0089 ± 0.1334	-0.1067 ± 0.0848	-0.0964 ± 0.0841
b_0^f	0.0108 ± 0.0002	0.0109 ± 0.0002	0.0106 ± 0.0002	0.0035 ± 0.0001	0.0036 ± 0.0001	0.0036 ± 0.0001
b_1^f	-0.0012 ± 0.0168	0.0081 ± 0.0101	0.0112 ± 0.0082	0.0041 ± 0.0036	0.0060 ± 0.0034	0.0059 ± 0.0032
b_2^f	-0.0379 ± 1.1507	0.0693 ± 0.2140	-0.0713 ± 0.1583	-0.0055 ± 0.0531	0.0287 ± 0.0447	0.0419 ± 0.0437
$b_1^{F_1}$	-0.0046 ± 0.0031	-0.0024 ± 0.0020	0.0015 ± 0.0014	0.0013 ± 0.0009	0.0013 ± 0.0008	0.0019 ± 0.0007
$b_2^{F_1}$	-0.0460 ± 0.1944	-0.0155 ± 0.0388	-0.0089 ± 0.0251	-0.0188 ± 0.0156	-0.0221 ± 0.0126	-0.0177 ± 0.0122
$b_1^{F_2}$	-0.2949 ± 0.0742	-0.2097 ± 0.0581	-0.1364 ± 0.0490	-0.0078 ± 0.0190	-0.0093 ± 0.0145	0.0001 ± 0.0136
$b_2^{F_2}$	0.5476 ± 4.0297	0.5667 ± 0.8789	0.5660 ± 0.7406	-0.2242 ± 0.1756	-0.1906 ± 0.1521	-0.1480 ± 0.1495
χ^2/dof	7.71/8	30.76/76	118.31/140	7.71/8	30.76/76	118.31/140
$R(D_q)$	0.3004 ± 0.0143	0.3066 ± 0.0081	0.2986 ± 0.0042	0.2993 ± 0.0046	0.2996 ± 0.0045	0.2971 ± 0.0042
$R(D_q^*)$	0.2718 ± 0.0300	0.2585 ± 0.0054	0.2500 ± 0.0016	0.2488 ± 0.0058	0.2506 ± 0.0040	0.2461 ± 0.0024

form factors at $\omega = \{1.00, 1.08, 1.16\}$ from the FNAL/MILC Collaboration [35] and the synthetic data points at $\omega = \{1.01, 1.06\}$ from the HPQCD analysis [36], (iii) the unquenched lattice results for the $\bar{B} \to D^*$ form factors at $\omega = \{1.03, 1.10, 1.17\}$ from the FNAL/MILC Collaboration [37], (iv) the lattice determinations of the $\bar{B}_s \to D_s$ form factors at $\omega = \{1.0, 1.06, 1.12\}$ from the HPQCD analysis [39], and (v) the lattice computations of the $\bar{B}_s \to D_s^*$ form factors at $\omega = \{1.0, 1.04, 1.08\}$ [40], we display in Table I the z-series coefficients from the BGL fitting with the truncation $n = 3$. In order to understand the significance of including the LCSR results in the BGL fit, we further carry out an alternative fit to the "only lattice QCD" data points of the $\bar{B}_q \to D_q^{(*)}$ form factors [35–37,39,40]. It needs to be stressed that our major objective is to investigate whether the inclusion of the large-recoil LCSR data points in the BGL fit strategy allows us to increase effectively the precision of the yielding form factors. It is evident from Fig. 2 that including the LCSR results is indeed highly beneficial for pining down the form-factor uncertainties at small q^2. As the third fit model, we also perform the statistical analysis by including the experimental data points together with the lattice QCD results and the LCSR predictions.

We proceed to present the correlated predictions for $\mathcal{R}(D)$ and $\mathcal{R}(D^*)$ in Fig. 3, confronted with the measurements from the *BABAR* [103,104], Belle [105–107], LHCb [108,109], and Belle II Collaborations [110]. Importantly, our determinations of $\mathcal{R}(D)$ and $\mathcal{R}(D^*)$ by encompassing the LCSR results in the numerical fit deviate from the HFLAV-averaged measurements by approximately 2.6σ, in contrast with the 3.3σ discrepancy between the arithmetic average of the previous SM predictions [48,49,111] and the state-of-the-art experimental average [13]. We further perform the simultaneous fit for $|V_{cb}|$ and $|V_{ub}|$ by taking the determined $\bar{B}_{(s)} \to D_{(s)}^{(*)}$ form factors and the predicted $\bar{B} \to \pi$ form factors [46] in combination with the lattice results for the $\bar{B}_{(s)} \to D_{(s)}^{(*)}$ form factors [35–37,39,40] and for the $\bar{B} \to \pi$ form factors [112–114] and the experimental measurements for $\bar{B}_{(s)} \to D_{(s)}^{(*)} \ell \bar{\nu}_\ell$ [1,3–5] and for $\bar{B} \to \pi \ell \bar{\nu}_\ell$ [115–119]. The yielding intervals of $|V_{cb}|$ and $|V_{ub}|$ are

$$\{|V_{cb}|, |V_{ub}|\} = \{(39.64 \pm 0.63), (3.71 \pm 0.13)\} \times 10^{-3}, \quad (6)$$

which coincide with the previous exclusive extractions for $|V_{cb}|$ [47–53,120–124]) and for $|V_{ub}|$ [91,125–127]. In an attempt to understand qualitatively the systematic uncertainties due to the truncated BGL expansions, we increase the expansion order to $n = 4$ and repeat the numerical fit procedure for the form factors, yielding the theory predictions for both the LFU ratios $\mathcal{R}(D^{(*)})$ and the CKM matrix elements $|V_{cb}|$ and $|V_{ub}|$ only marginally different from the achieved results with $n = 3$.

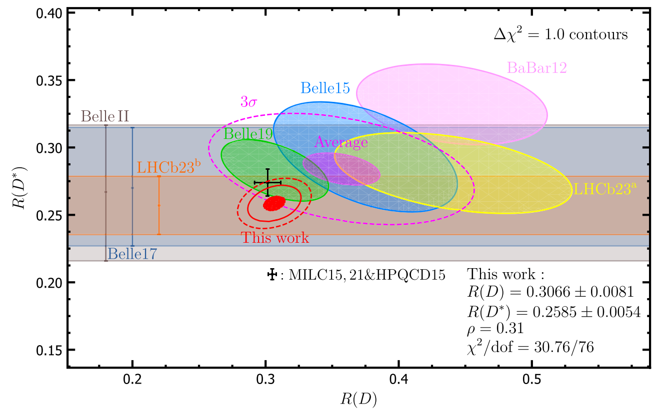

FIG. 3. The correlated predictions for $\mathcal{R}(D)$ and $\mathcal{R}(D^*)$ from the combined BGL fits against the lattice data points [35–37] and the NLL $\oplus$ NLP LCSR predictions. The available measurements from the *BABAR* [103,104], Belle [105–107], LHCb [108,109], and Belle II Collaborations [110] are also displayed.

V. CONCLUSIONS

In conclusion, we have endeavored to accomplish for the first time the complete next-to-leading-order QCD computations of the $\bar{B}_q \to D_q^{(*)} \ell \bar{\nu}_\ell$ form factors at large recoil and identified explicitly the unsuppressed charm-quark-mass dependent contributions in the heavy quark expansion. Taking into account the obtained LCSR data points in the BGL z-series fit of the $\bar{B}_q \to D_q^{(*)} \ell \bar{\nu}_\ell$ form factors enabled us to enhance significantly the achieved accuracy of the large-recoil theory predictions for the $\bar{B} \to D^{(*)}$ form factors. Implementing the determined LCSR results in the statistical analysis turned out to be advantageous to mitigate the combined $\mathcal{R}(D)$ and $\mathcal{R}(D^*)$ tension between the SM predictions and the HFLAV-averaged measurements.

ACKNOWLEDGMENTS

We are grateful to Thomas Mannel, Zi-Hao Mi, Ru-Ying Tang, Alejandro Vaquero, Chao Wang, and Yan-Bing Wei for illuminating discussions. Y. M. W. acknowledges support from the National Natural Science Foundation of China with Grants No. 11735010 and No. 12075125, and the Natural Science Foundation of Tianjin with Grant No. 19JCJQJC61100.

[1] R. Glattauer *et al.* (Belle Collaboration), Phys. Rev. D **93**, 032006 (2016).
[2] A. Abdesselam *et al.* (Belle Collaboration), arXiv: 1702.01521.
[3] E. Waheed *et al.* (Belle Collaboration), Phys. Rev. D **100**, 052007 (2019); **103**, 079901(E) (2021).
[4] R. Aaij *et al.* (LHCb Collaboration), Phys. Rev. D **101**, 072004 (2020).
[5] R. Aaij *et al.* (LHCb Collaboration), J. High Energy Phys. 12 (2020) 144.
[6] M. T. Prim *et al.* (Belle Collaboration), Phys. Rev. D **108**, 012002 (2023).
[7] W. Altmannshofer *et al.* (Belle-II Collaboration), Prog. Theor. Exp. Phys. **2019**, 123C01 (2019); **2020**, 029201(E) (2020).
[8] P. Gambino *et al.*, Eur. Phys. J. C **80**, 966 (2020).
[9] P. A. Boyle *et al.*, in 2022 Snowmass Summer Study (2022), arXiv:2205.15373.
[10] A. S. Kronfeld *et al.* (USQCD Collaboration), arXiv: 2207.07641.
[11] A. Di Canto and S. Meinel, arXiv:2208.05403.
[12] F. U. Bernlochner, M. F. Sevilla, D. J. Robinson, and G. Wormser, Rev. Mod. Phys. **94**, 015003 (2022).
[13] Y. Amhis *et al.* (HFLAV Collaboration), Phys. Rev. D **107**, 052008 (2023).
[14] F. U. Bernlochner and Z. Ligeti, Phys. Rev. D **95**, 014022 (2017).
[15] F. U. Bernlochner, Z. Ligeti, D. J. Robinson, and W. L. Sutcliffe, Phys. Rev. Lett. **121**, 202001 (2018).
[16] T. D. Cohen, H. Lamm, and R. F. Lebed, Phys. Rev. D **98**, 034022 (2018).
[17] N. Das and R. Dutta, Phys. Rev. D **105**, 055027 (2022).
[18] N. Gubernari, A. Khodjamirian, R. Mandal, and T. Mannel, J. High Energy Phys. 05 (2022) 029.
[19] F. U. Bernlochner, Z. Ligeti, M. Papucci, and D. J. Robinson, Phys. Rev. D **107**, L011502 (2023).
[20] S. Patnaik and R. Singh, Universe **9**, 129 (2023).
[21] S. Patnaik, L. Nayak, and R. Singh, arXiv:2308.05677.
[22] N. Penalva, J. M. Flynn, E. Hernández, and J. Nieves, arXiv:2304.00250.
[23] R. Aaij *et al.* (LHCb Collaboration), Phys. Rev. Lett. **131**, 051803 (2023).
[24] R. Aaij *et al.* (LHCb Collaboration), Phys. Rev. D **108**, 032002 (2023).
[25] N. R. Singh Chundawat, Phys. Rev. D **107**, 055004 (2023).
[26] A. K. Alok, N. R. Singh Chundawat, and A. Mandal, arXiv:2303.16606.
[27] M. Algueró, A. Biswas, B. Capdevila, S. Descotes-Genon, J. Matias, and M. Novoa-Brunet, Eur. Phys. J. C **83**, 648 (2023).
[28] R. Fleischer, E. Malami, A. Rehult, and K. K. Vos, J. High Energy Phys. 06 (2023) 033.
[29] C. G. Boyd, B. Grinstein, and R. F. Lebed, Phys. Lett. B **353**, 306 (1995).
[30] C. G. Boyd, B. Grinstein, and R. F. Lebed, Nucl. Phys. **B461**, 493 (1996).
[31] C. G. Boyd, B. Grinstein, and R. F. Lebed, Phys. Rev. D **56**, 6895 (1997).
[32] I. Caprini and C. Macesanu, Phys. Rev. D **54**, 5686 (1996).
[33] I. Caprini, L. Lellouch, and M. Neubert, Nucl. Phys. **B530**, 153 (1998).
[34] C. Bourrely, I. Caprini, and L. Lellouch, Phys. Rev. D **79**, 013008 (2009); **82**, 099902(E) (2010).
[35] J. A. Bailey *et al.* (MILC Collaboration), Phys. Rev. D **92**, 034506 (2015).
[36] H. Na, C. M. Bouchard, G. P. Lepage, C. Monahan, and J. Shigemitsu (HPQCD Collaboration), Phys. Rev. D **92**, 054510 (2015); **93**, 119906(E) (2016).
[37] A. Bazavov *et al.* (Fermilab Lattice, MILC Collaboration), Eur. Phys. J. C **82**, 1141 (2022).
[38] J. A. Bailey *et al.*, Phys. Rev. D **85**, 114502 (2012); **86**, 039904(E) (2012).
[39] E. McLean, C. T. H. Davies, J. Koponen, and A. T. Lytle, Phys. Rev. D **101**, 074513 (2020).
[40] J. Harrison and C. T. H. Davies (HPQCD Collaboration), Phys. Rev. D **105**, 094506 (2022).
[41] S. Faller, A. Khodjamirian, C. Klein, and T. Mannel, Eur. Phys. J. C **60**, 603 (2009).
[42] N. Gubernari, A. Kokulu, and D. van Dyk, J. High Energy Phys. 01 (2019) 150.
[43] Y.-M. Wang, Y.-B. Wei, Y.-L. Shen, and C.-D. Lü, J. High Energy Phys. 06 (2017) 062.
[44] J. Gao, T. Huber, Y. Ji, C. Wang, Y.-M. Wang, and Y.-B. Wei, J. High Energy Phys. 05 (2022) 024.
[45] M. C. Arnesen, B. Grinstein, I. Z. Rothstein, and I. W. Stewart, Phys. Rev. Lett. **95**, 071802 (2005).
[46] B.-Y. Cui, Y.-K. Huang, Y.-L. Shen, C. Wang, and Y.-M. Wang, J. High Energy Phys. 03 (2023) 140.
[47] D. Bigi, P. Gambino, and S. Schacht, J. High Energy Phys. 11 (2017) 061.
[48] P. Gambino, M. Jung, and S. Schacht, Phys. Lett. B **795**, 386 (2019).
[49] M. Bordone, M. Jung, and D. van Dyk, Eur. Phys. J. C **80**, 74 (2020).
[50] M. Bordone, N. Gubernari, D. van Dyk, and M. Jung, Eur. Phys. J. C **80**, 347 (2020).
[51] S. Jaiswal, S. Nandi, and S. K. Patra, J. High Energy Phys. 12 (2017) 060.
[52] S. Jaiswal, S. Nandi, and S. K. Patra, J. High Energy Phys. 06 (2020) 165.
[53] A. Biswas, S. Nandi, and I. Ray, J. High Energy Phys. 07 (2023) 024.
[54] K. Cheung, Z.-R. Huang, H.-D. Li, C.-D. Lü, Y.-N. Mao, and R.-Y. Tang, Nucl. Phys. **B965**, 115354 (2021).
[55] H. Boos, T. Feldmann, T. Mannel, and B. D. Pecjak, Phys. Rev. D **73**, 036003 (2006).
[56] H. Boos, T. Feldmann, T. Mannel, and B. D. Pecjak, J. High Energy Phys. 05 (**2006**) 056.
[57] J. Gao, C.-D. Lü, Y.-L. Shen, Y.-M. Wang, and Y.-B. Wei, Phys. Rev. D **101**, 074035 (2020).
[58] See Supplemental Material at http://link.aps.org/supplemental/10.1103/PhysRevD.108.L071504 for the explicit expressions of the considered SCET form factors and the detailed numerical results of the exclusive heavy-to-heavy form factors.
[59] M. Beneke and D. Yang, Nucl. Phys. **B736**, 34 (2006).
[60] M. Beneke, Y. Kiyo, and D. s. Yang, Nucl. Phys. **B692**, 232 (2004).

[61] R. J. Hill, T. Becher, S. J. Lee, and M. Neubert, J. High Energy Phys. 07 (2004) 081.
[62] F. De Fazio, T. Feldmann, and T. Hurth, Nucl. Phys. **B733**, 1 (2006); **B800**, 405(E) (2008).
[63] F. De Fazio, T. Feldmann, and T. Hurth, J. High Energy Phys. 02 (2008) 031.
[64] A. Khodjamirian, T. Mannel, and N. Offen, Phys. Lett. B **620**, 52 (2005).
[65] A. Khodjamirian, T. Mannel, and N. Offen, Phys. Rev. D **75**, 054013 (2007).
[66] M. Beneke and T. Feldmann, Phys. Lett. B **553**, 267 (2003).
[67] A. K. Leibovich, Z. Ligeti, and M. B. Wise, Phys. Lett. B **564**, 231 (2003).
[68] P. Böer, QCD factorisation in exclusive semileptonic B decays: New applications and resummation of rapidity logarithms, Ph.D. thesis, University of Siegen, https://dspace.ub.uni-siegen.de/handle/ubsi/1369, 2018.
[69] M. Beneke, V. M. Braun, Y. Ji, and Y.-B. Wei, J. High Energy Phys. 07 (2018) 154.
[70] G. Bell, T. Feldmann, Y.-M. Wang, and M. W. Y. Yip, J. High Energy Phys. 11 (**2013**) 191.
[71] Y.-M. Wang and Y.-L. Shen, Nucl. Phys. **B898**, 563 (2015).
[72] Y.-M. Wang, J. High Energy Phys. 09 (2016) 159.
[73] Y.-M. Wang and Y.-L. Shen, J. High Energy Phys. 05 (2018) 184.
[74] Y.-L. Shen, Y.-M. Wang, and Y.-B. Wei, J. High Energy Phys. 12 (2020) 169.
[75] C. Wang, Y.-M. Wang, and Y.-B. Wei, J. High Energy Phys. 02 (2022) 141.
[76] T. Feldmann, P. Lüghausen, and D. van Dyk, J. High Energy Phys. 10 (2022) 162.
[77] V. M. Braun, D. Y. Ivanov, and G. P. Korchemsky, Phys. Rev. D **69**, 034014 (2004).
[78] A. Khodjamirian, R. Mandal, and T. Mannel, J. High Energy Phys. 10 (2020) 043.
[79] A. G. Grozin and M. Neubert, Phys. Rev. D **55**, 272 (1997).
[80] T. Nishikawa and K. Tanaka, Nucl. Phys. **B879**, 110 (2014).
[81] M. Rahimi and M. Wald, Phys. Rev. D **104**, 016027 (2023).
[82] V. M. Braun, Y. Ji, and A. N. Manashov, J. High Energy Phys. 05 (2017) 022.
[83] W. Wang, Y.-M. Wang, J. Xu, and S. Zhao, Phys. Rev. D **102**, 011502 (2020).
[84] Y. Aoki *et al.* (flavor Lattice Averaging Group (FLAG)), Eur. Phys. J. C **82**, 869 (2022).
[85] B. Pullin and R. Zwicky, J. High Energy Phys. 09 (2021) 023.
[86] A. Khodjamirian, C. Klein, T. Mannel, and N. Offen, Phys. Rev. D **80**, 114005 (2009).
[87] G. Duplancic and B. Melic, J. High Energy Phys. 11 (2015) 138.
[88] H.-D. Li, C.-D. Lü, C. Wang, Y.-M. Wang, and Y.-B. Wei, J. High Energy Phys. 04 (2020) 023.
[89] A. Khodjamirian, B. Melić, Y.-M. Wang, and Y.-B. Wei, J. High Energy Phys. 03 (**2021**) 016.
[90] I. Sentitemsu Imsong, A. Khodjamirian, T. Mannel, and D. van Dyk, J. High Energy Phys. 02 (2015) 126.
[91] D. Leljak, B. Melić, and D. van Dyk, J. High Energy Phys. 07 (2021) 036.
[92] B. Chibisov, R. D. Dikeman, M. A. Shifman, and N. Uraltsev, Int. J. Mod. Phys. A **12**, 2075 (1997).
[93] M. A. Shifman, in *8th International Symposium on Heavy Flavor Physics* (World Scientific, Singapore, 2000), Vol. 3, pp. 1447–1494; arXiv:hep-ph/0009131.
[94] I. I. Y. Bigi and N. Uraltsev, Int. J. Mod. Phys. A **16**, 5201 (2001).
[95] O. Cata, M. Golterman, and S. Peris, J. High Energy Phys. 08 (2005) 076.
[96] M. Beylich, G. Buchalla, and T. Feldmann, Eur. Phys. J. C **71**, 1635 (2011).
[97] M. Jamin, J. High Energy Phys. 09 (2011) 141.
[98] J. Dingfelder and T. Mannel, Rev. Mod. Phys. **88**, 035008 (2016).
[99] D. Boito, I. Caprini, M. Golterman, K. Maltman, and S. Peris, Phys. Rev. D **97**, 054007 (2018).
[100] A. Pich, Prog. Part. Nucl. Phys. **117**, 103846 (2021).
[101] A. Pich and A. Rodríguez-Sánchez, J. High Energy Phys. 07 (2022) 145.
[102] D. Bigi, P. Gambino, and S. Schacht, Phys. Lett. B **769**, 441 (2017).
[103] J. P. Lees *et al.* (*BABAR* Collaboration), Phys. Rev. Lett. **109**, 101802 (2012).
[104] J. P. Lees *et al.* (*BABAR* Collaboration), Phys. Rev. D **88**, 072012 (2013).
[105] M. Huschle *et al.* (Belle Collaboration), Phys. Rev. D **92**, 072014 (2015).
[106] G. Caria *et al.* (Belle Collaboration), Phys. Rev. Lett. **124**, 161803 (2020).
[107] S. Hirose *et al.* (Belle Collaboration), Phys. Rev. Lett. **118**, 211801 (2017).
[108] R. Aaij *et al.* (LHCb Collaboration), Phys. Rev. Lett. **131**, 111802 (2023).
[109] R. Aaij *et al.* (LHCb Collaboration), Phys. Rev. D **108**, 012018 (2023).
[110] K. Kojima *et al.* (Belle II Collaboration), *Talk Presented at the Lepton Photon Conference* (2023), https://indico.cern.ch/event/1114856/contributions/5423684/.
[111] D. Bigi and P. Gambino, Phys. Rev. D **94**, 094008 (2016).
[112] J. M. Flynn, T. Izubuchi, T. Kawanai, C. Lehner, A. Soni, R. S. Van de Water, and O. Witzel, Phys. Rev. D **91**, 074510 (2015).
[113] J. A. Bailey *et al.* (Fermilab Lattice, MILC Collaboration), Phys. Rev. D **92**, 014024 (2015).
[114] J. A. Bailey *et al.* (Fermilab Lattice, MILC Collaboration), Phys. Rev. Lett. **115**, 152002 (2015).
[115] P. del Amo Sanchez *et al.* (*BABAR* Collaboration), Phys. Rev. D **83**, 032007 (2011).
[116] J. P. Lees *et al.* (*BABAR* Collaboration), Phys. Rev. D **86**, 092004 (2012).
[117] H. Ha *et al.* (Belle Collaboration), Phys. Rev. D **83**, 071101 (2011).
[118] A. Sibidanov *et al.* (Belle Collaboration), Phys. Rev. D **88**, 032005 (2013).
[119] K. Adamczyk *et al.* (Belle-II Collaboration), arXiv:2210.04224.

[120] B. Grinstein and A. Kobach, Phys. Lett. B **771**, 359 (2017).

[121] G. Martinelli, S. Simula, and L. Vittorio, Phys. Rev. D **105**, 034503 (2022).

[122] G. Martinelli, S. Simula, and L. Vittorio, Eur. Phys. J. C **82**, 1083 (2022).

[123] G. Martinelli, M. Naviglio, S. Simula, and L. Vittorio, Phys. Rev. D **106**, 093002 (2022).

[124] S. Iguro and R. Watanabe, J. High Energy Phys. 08 (2020) 006.

[125] A. Biswas, S. Nandi, S. K. Patra, and I. Ray, J. High Energy Phys. 07 (2021) 082.

[126] A. Biswas and S. Nandi, J. High Energy Phys. 09 (2021) 127.

[127] G. Martinelli, S. Simula, and L. Vittorio, J. High Energy Phys. 08 (2022) 022.